# THE GEM DETECTOR PROJECTIVE ALIGNMENT SIMULATION SYSTEM

*Craig R. Wuest, F. Curtis Belser, Fred R. Holdener, Martin D. Roeben*
*Lawrence Livermore National Laboratory, Livermore, California, USA*

*Joseph A. Paradiso*
*Charles Stark Draper Laboratory, Cambridge, Massachusetts, USA*

*Gena Mitselmakher, Andrei Ostapchuk, Jacques Pier-Amory*
*Superconducting Supercollider Laboratory, Dallas, TX, USA*

## 1. INTRODUCTION

Precision position knowledge (< 25 microns RMS) of the GEM Detector muon system at the Superconducting Super Collider Laboratory (SSCL) is an important physics requirement necessary to minimize sagitta error in detecting and tracking high energy muons that are deflected by the magnetic field within the GEM Detector. To validate the concept of the sagitta correction function determined by projective alignment of the muon detectors (Cathode Strip Chambers or CSCs), the basis of the proposed GEM alignment scheme, a facility, called the "Alignment Test Stand" (ATS), is being constructed [1]. This system simulates the environment that the CSCs and chamber alignment systems are expected to experience in the GEM Detector, albeit without the 0.8 T magnetic field and radiation environment. The ATS experimental program will allow systematic study and characterization of the projective alignment approach, as well as general mechanical engineering of muon chamber mounting concepts, positioning systems and study of the mechanical behavior of the proposed 6 layer CSCs. The ATS will consist of a stable local coordinate system in which mock-ups of muon chambers *(i.e.,* non-working mechanical analogs, representing the three superlayers of a selected barrel and endcap alignment tower) are implemented, together with a sufficient number of alignment monitors to overdetermine the sagitta correction function, providing a self-consistency check. This paper describes the approach to be used for the alignment of the GEM muon system, the design of the ATS, and the experiments to be conducted using the ATS.

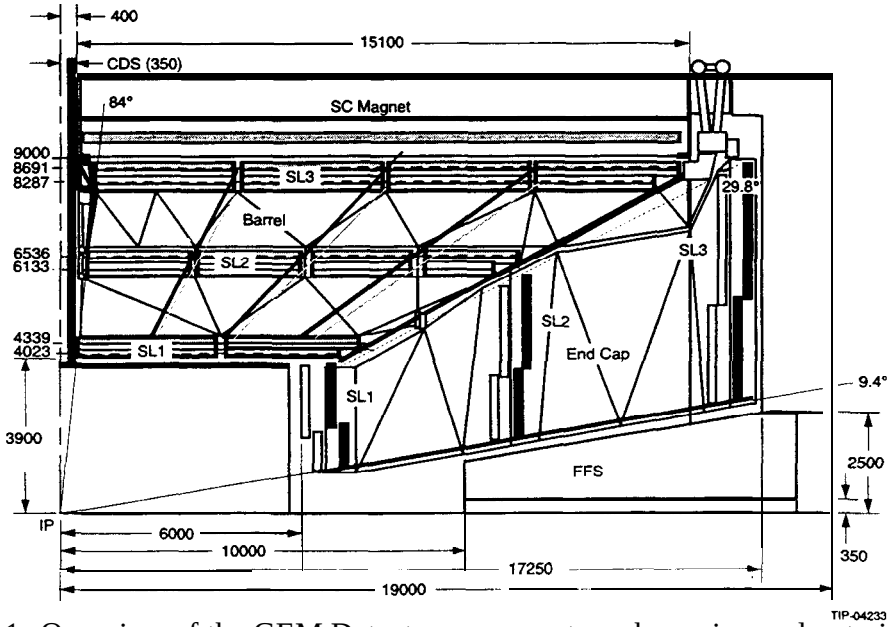


Fig. 1 Overview of the GEM Detector muon system shown in quadrant view

Figure 1 shows the layout of the GEM Detector muon system. The muon system consists of chambers arranged in projective alignment towers defined by lines of sight at the ends of each chamber. The ATS is designed to simulate a single phi sector of the first barrel tower from a polar angle ($\theta$) of approximately 84° to 62°, and the first endcap tower, $\theta \approx$ 18° to 10°. The mock chambers will be kinematically mounted with positioning actuators used to place the chambers to within the dynamic range of the alignment system. Chambers will be fitted with precision alignment fixtures containing a light source, lens, or detector, for inner, middle, and outer superlayer chambers, respectively. A series of tests will be conducted whereby the redundant alignment monitors will be checked for self-consistency, as well as compared with a precise external alignment system.

## 2. THE GEM DETECTOR ALIGNMENT PHILOSOPHY

The GEM muon system is aligned locally within a specially configured projective tower formed as a part of the CSC chamber layout, as well as globally with respect to the interaction point (IP). The discussion below describes the local alignment between superlayers, which directly impacts the momentum resolution and is quite stringent. Table 1 summarizes the local alignment and positioning tolerances for the GEM muon system. The GEM muon system measures the trajectory of a muon track in three roughly equidistant superlayers. The deviation of these measured points from a straight line (sagitta) determines the track curvature, and hence the muon momentum. The bending coordinate misalignment of chamber superlayers must be limited to $\pm 25\mu m$ in order to retain the desired momentum resolution of the GEM muon detector (momentum resolution for 500 GeV $p_T$: $\Delta p_T/p_T \approx$ 5% at $|\eta| \approx 0$ and $\Delta p_T/p_T \approx$ 12% at $|\eta| = 2.5$). If the three superlayers are misaligned along the muon bending direction, a false sagitta will result, leading to errors in the momentum measurement.

To maintain this precision, each tower will be instrumented to dynamically monitor the relative alignment of its composite CSC superlayers, as shown in Figure 2. These local alignment systems are based on modified and updated versions of the three-point optical straightness monitors used at the L3 detector at CERN [2], which directly measure the deviation of 3 points

**Table 1**

Requirements and resolutions assumed for local alignment

| *Contributing to Momentum Resolution* | | | |
|---|---|---|---|
| Relative superlayer positioning (wrt inner superlayer) | Middle superlayer | Δx<br>Δy<br>Δz<br>Rx<br>Ry<br>Rz | ± 1.5 mm<br>± 1.5 mm<br>± 1.5 mm<br>± 1 mrad<br>± 1 mrad<br>± 3 mrad |
| Relative superlayer positioning (wrt inner superlayer) | Outer superlayer | Δx<br>Δy<br>Δz<br>Rx<br>Ry<br>Rz | ± 3 mm<br>± 3 mm<br>± 3 mm<br>± 1.5. mrad<br>± 1.5 mrad<br>± 5. mrad |
| Chamber flatness | All layers | Random Bumps<br>Maximum Sag | $\sigma$ = 100 $\mu$m<br>< 200 $\mu$m |
| Monitor positioning | Inner, outer<br>middle | Δx<br>Δx | ± 20 $\mu$m<br>± 10 $\mu$m |
| Monitor resolution | Measurement error | $\sigma$ | 25 $\mu$m |
| Line–of-sight projectivity | From global alignment | Δρ<br>Δζ | ± 3 cm<br>± 3 cm |
| θ-Coordinate Resolution | In each tower | $\sigma$ | 3 mrad |
| *Limits from Other Sources (wrt outer superlayer)* | | | |
| Trigger projectivity | Middle superlayer | Δx | ± 5 mm |
| Dynamic range of monitors | Middle superlayer<br>Inner superlayer | Δx, Δz<br>Δx, Δz | ± 5 mm<br>± 1 cm |

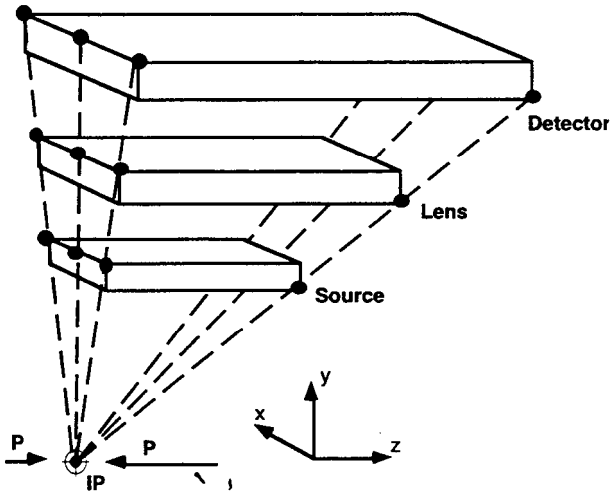


Fig. 2 Projective alignment tower

from a straight line. Figure 3 shows the implementation of the 3-point straightness monitor proposed for GEM based on video cameras imaging 2-dimensional coded masks [3].

It has been determined that superlayer misalignments will produce sagitta errors that may be described to sufficient accuracy by a quadratic in the tangent of the local $\phi$ angle (where $\phi = 0$ at the center of the tower) for high-momentum muon tracks originating at the IP. By measuring the chamber misalignment in the local projective $\phi$ coordinate at three points across the $\phi$-width of the tower, a quadratic function is determined that can precisely interpolate a sagitta correction. Running 3-point monitor arrays along both sides of a projective tower, as depicted in Fig. 2, allows a quadratic interpolation in the $\phi$ coordinate and a linear interpolation in the $\theta$ coordinate of a muon track. This quadratic interpolation can be used to compensate the sagitta errors caused by superlayer misalignments. Only 5 out of 6 monitors are required to track rigid-body displacements and uniform thermal expansion, providing a degree of fault tolerance. If all six monitors are utilized, "torque" errors, where opposite edges of elastic chambers are differentially twisted and/or stretched, are also suppressed by the correction method [4].

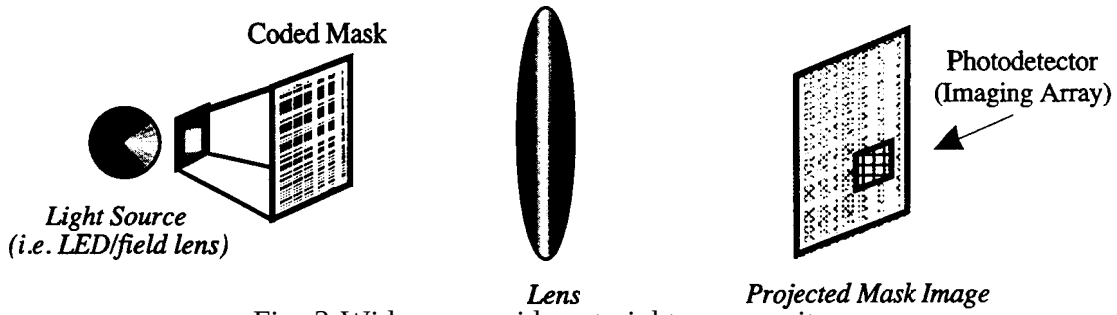


Fig. 3 Wide-range video straightness monitor

Figures 4 and 5 identify the projective alignment paths for barrel and endcap towers. The barrel arrangement is as described above, however the endcap utilizes a more complex arrangement of projective and radial paths. Each endcap tower will have 3 projective alignment paths along its top edge (high $\theta$) and two alignment paths along its lower edge (low $\theta$). In order to attain complete acceptance coverage, however, the upper and lower endcap chamber packages are overlapped in $\theta$, preventing a line of sight from traversing their inner edges. To overcome this difficulty, the upper and lower sets of chambers are rigidly coupled together at the point of overlap, thereby mechanically transferring the projective alignment measurements between the top and bottom 3-point paths, and forming complete alignment towers. A set of radial straightness monitors will be directed along the $\phi$-edges of each linked chamber package, with the LED light source at bottom, lens at the point, where the upper/lower chambers are joined, and photodetector at top (Fig. 5, side views). These will monitor the relative $\phi$ and $z$ deflections of upper and lower endcap segments. Note that only two projective alignment paths are prescribed for the smallest $\theta$ edge of the endcap, as opposed to the three implemented elsewhere that are needed to reconstruct the quadratic sagitta error function. Because the projective lines-of-sight are much closer together at small $\theta$, the sagitta errors are much less sensitive to z-translations and y-rotations there, thus the need for three alignment paths is relaxed

Quadratic interpolation has been demonstrated by simulation and analysis [4,5]. The effect of the alignment correction is demonstrated in Fig. 6. The plot on the left shows the false sagitta injected into a straight-line muon track traversing the first barrel $\theta$-section alignment

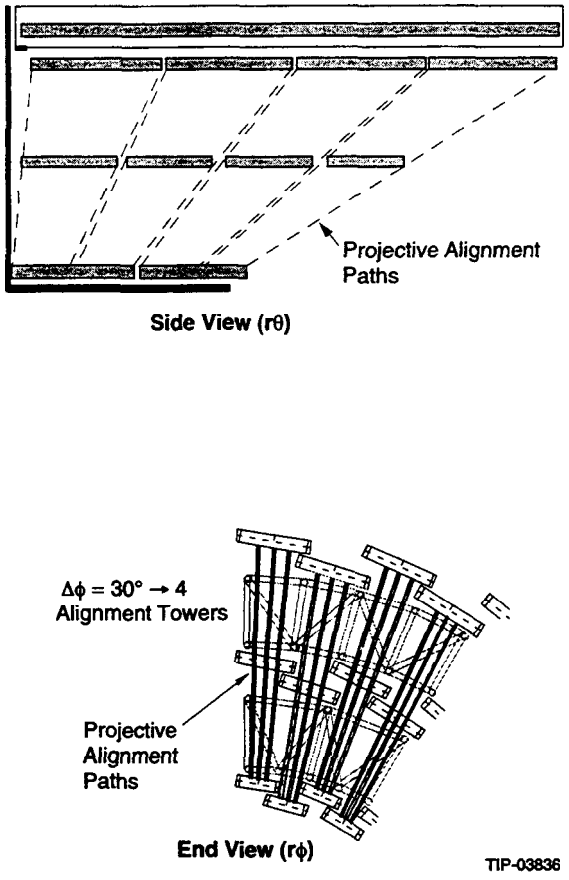


Fig. 4 Barrel projective lines-of-sight

tower with the superlayers rotated and translated away from their nominal positions as a function of the muon angles $\theta$ and $\phi$. Because of the chamber displacements, the sagitta error ranges up to 4 mm in this example, with an average error magnitude of 1.1 mm, which is certainly unacceptable. The right-hand plot shows the false sagitta after the alignment interpolation correction has been applied [5]. The surface is now of higher order (the quadratic dependence being removed), and error ranges between ± 10 $\mu$m with an average 5 $\mu$m, which is well within our allowed tolerance.

The analysis effort of Ref. [6] has examined these post-correction sagitta residuals for random chamber displacements, resulting in the local chamber positioning requirements of Figure 7 and Table 1. These are the maximum permissible superlayer rotations and translations both relative to the inner superlayer over which the sagitta errors are adequately removed. The error sources quoted for local alignment in Table 1 trade off against one another *(i.e.,* tightening one allows another to loosen); they have been selected to contribute roughly an equal amount of about 10 $\mu$m in quadrature to the net 25 $\mu$m error budget [6]. In addition, a $z$-coordinate resolution yielding $\sigma_\theta$ = 3 mrad has been assumed in this analysis the $\theta$-

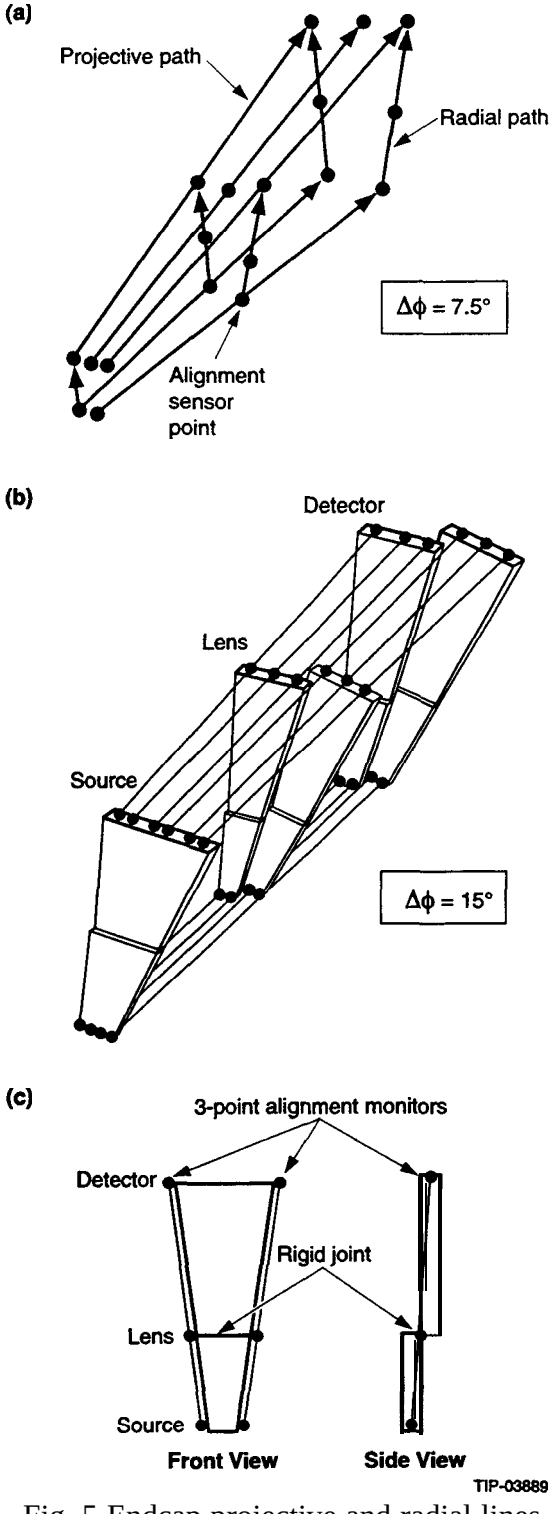


Fig. 5 Endcap projective and radial lines-of-sight

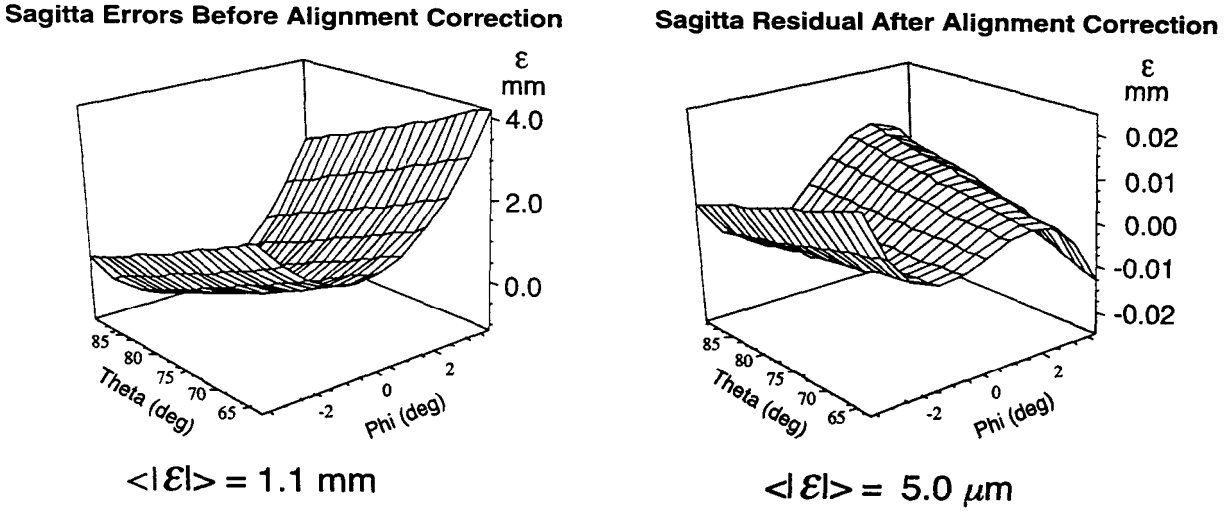


FIG. 6 Sagitta errors in a projective alignment tower before and after alignment correction

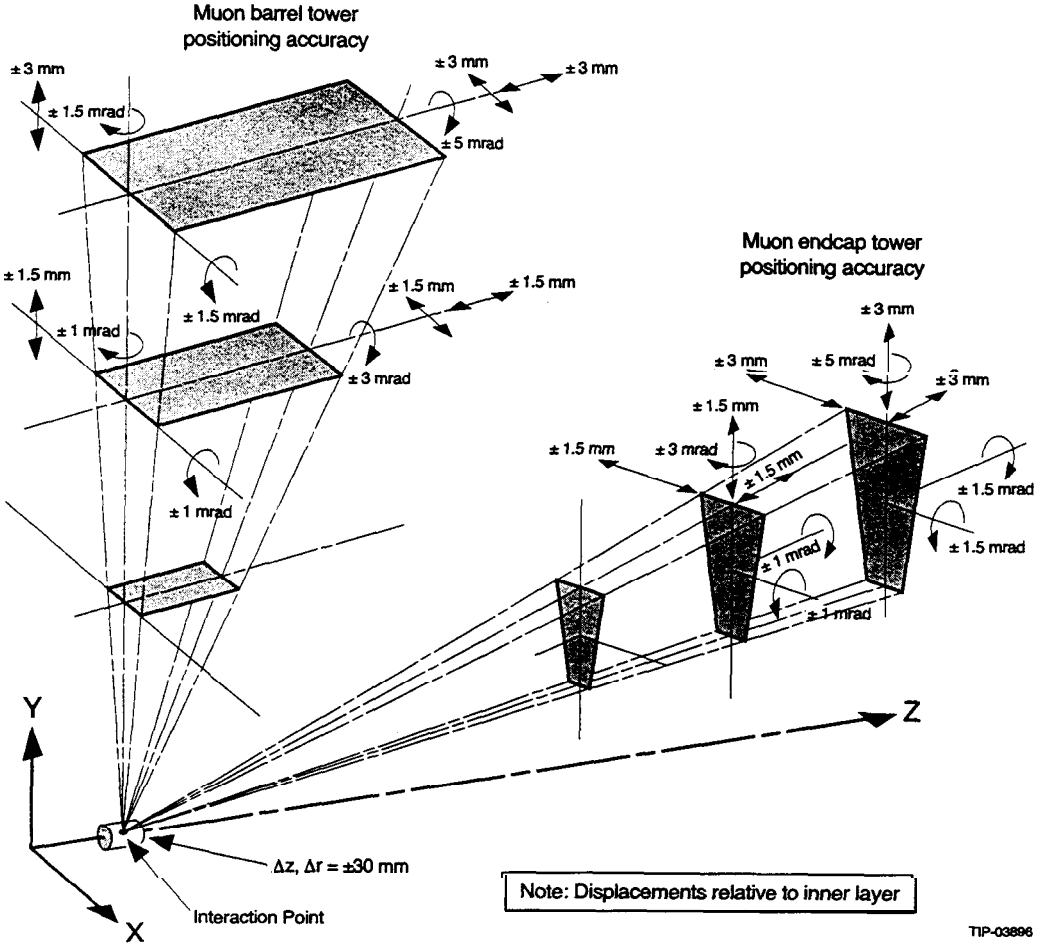


FIG. 7 Maximum allowed local deflections and rotations in an alignment tower

measurement is needed for the interpolation between monitor triads, thus this resolution likewise contributes to the alignment error. Studies show that the net residual after alignment correction for straight-line tracks emanating from the interaction diamond (the locus of beam crossings in the region of the IP), assuming simultaneous alignment errors statistically distributed within the limits of Table 1, maintains the $\sigma < 25$ $\mu$m error budgets. The stringent $\mu$m

and $\mu$rad positioning requirements that were previously imposed [7,8] are thus removed, provided the straightness monitor axes point toward the IP within a cylinder of ± 3 cm ($z$), and ± 3 cm ($r$) (see Figure 7). Arbitrary deflections up to several mm and rotations at the milliradian level may thus be compensated to produce an average sagitta residual within the 25 $\mu$m limit for stiff muon tracks coming from the IP. Although only the bending-coordinate misalignment need be measured to perform this correction, knowledge of the orthogonal (non-bending) coordinate will aid in fault tolerance[4] and prove useful in resolving positioning ambiguities, thereby increasing the range of sagitta correction [5]. Analysis of the actual muon data may likewise break the ambiguities in local chamber positioning, significantly expanding the limits of Table 1.

## 3. ALIGNMENT TEST STAND DESIGN

The Alignment Test Stand (Fig. 8) will consist of two major assemblies and will test proposed alignment component hardware for the barrel and endcap projective towers. The ATS chambers will simulate as closely as possible the actual size, stiffness and density (total weight to volume ratio) of the CSCs. The endcap ATS requires a configuration that is technically more challenging because the alignment distances are roughly twice that of the shorter barrel tower with the added complexity of non-rectangular CSCs. The framework for supporting both assemblies will be as rigid a structure as is practical, but for simplicity will not be the actual structure proposed for the GEM muon system. All CSC mock-ups, projective alignment components, and frames will be mounted to massive granite bases that are structurally and thermally stable. Connections to the granite bases will be made through a steel structural support assembly shown schematically in Fig. 9. CSC engineering mock-ups will be constructed with 5 internal holes and 8 fixture locations about the panel perimeters (4 corners, 4 edge-centers) for alignment hardware. The holes and fixtures will line up projectively across all dummy superlayers; the alignment monitors about the perimeter will determine the alignment interpolation correction, to be checked against the alignment monitors inside the panel boundary (simulating stiff muon tracks). Thus the alignment will be "over-determined" in order to fully validate the quadratic interpolation scheme described previously. Chamber mock-ups will be kinematically mounted to the steel structural supports using interface hardware that provides the required

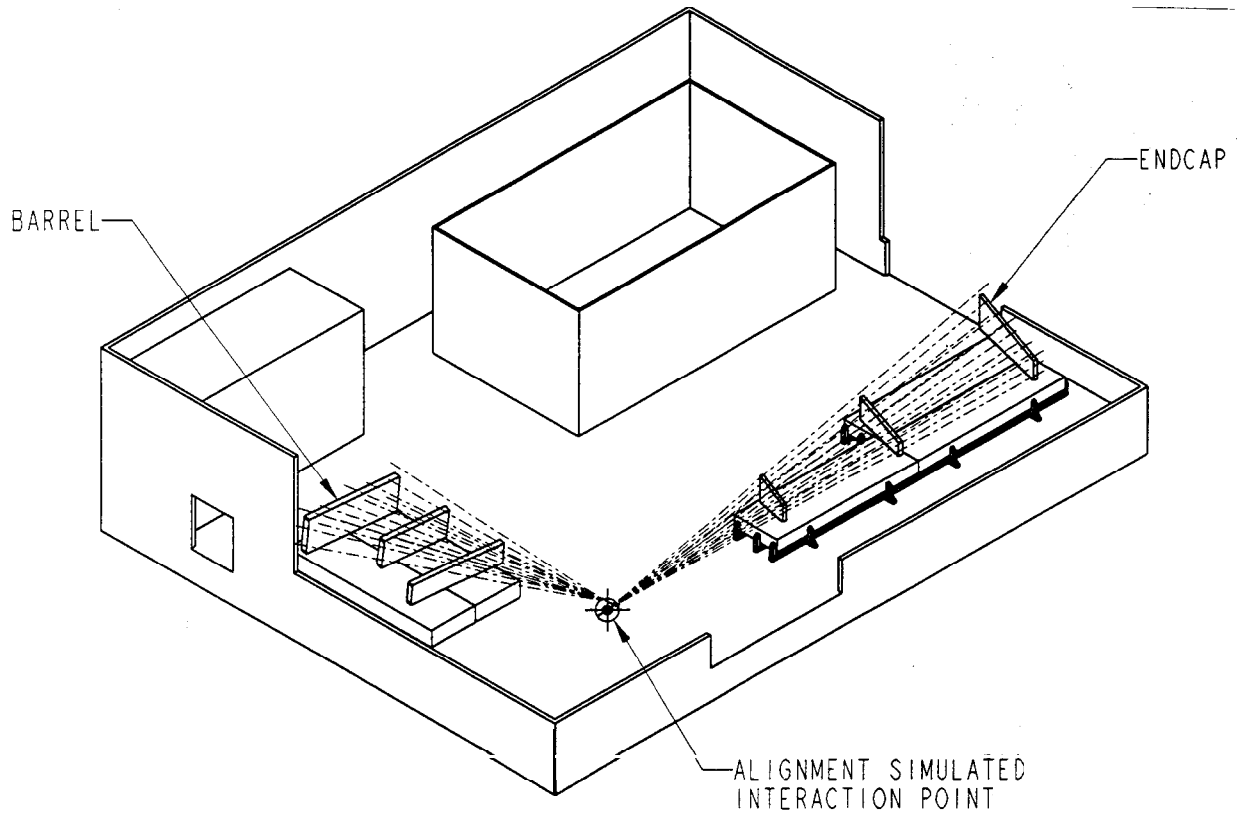


Fig. 8 Schematic representation of the ATS showing a barrel and endcap set of muon chambers

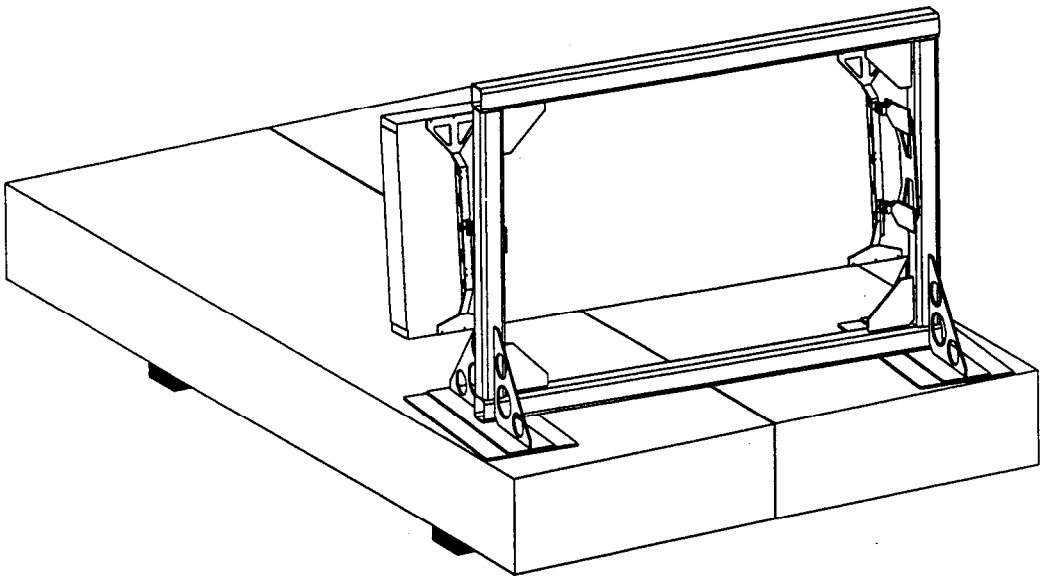

Fig. 9 Kinematic mounting of mock chamber to ATS support

translations and rotations for testing the proposed projective alignment system.

The goals for the ATS include the following: provide a test bed for proposed projective alignment hardware that enables measurements to be taken under the expected on-site environment; provide variable temperature conditions as would be seen at the detector; examine the effects due to air disturbances on the alignment measurements of an actual structure; evaluate the CSC structural deflections due to expected mechanical loadings (gravitational, vibrational, assembly, *etc.);* evaluate the impact of various alignment schemes on the actual structural hardware designs; provide a "test bed" for operational alignment procedure development, testing and certification; demonstrate the physical constraints on various alignment schemes; test positioning actuators and kinematic mounting schemes for the CSC-support structure interface.

## 4. ATS EXPERIMENTAL PROGRAM

Commissioning of the ATS is expected to take place in a hi-bay facility located at Lawrence Livermore National Laboratory. After commissioning, the ATS will be installed as a permanent user facility at SSCL. Initial alignment of all test articles and support frames will use crosshairs and a theodolite system with accompanying computer system. Past experience with this system indicates targets can be aligned to within the 50 to 100 micron range, well within the specification of 1 to 2 mm initial alignment for CSCs. One of the theodolites will be mounted at the simulated detector IP with respect to the CSCs and another approximately 5 meters off to the side, while keeping all targets within sight. The CSCs will be individually adjusted to be at their ideal desired coordinates. The alignment fixtures will be simple mounting blocks with the correct LOS (projective "line of sight") angle machined into them. A single adjustment fixture will be designed to allow precision movement of the individual holders to position them before being firmly fastened in place with locking screws. A standardized barrel attachment with a precision fit diameter and plane surface will be used at all locations for mounting all LOS alignment elements.

Once all the LOS have been aligned and locked in place using the theodolite system, the projective alignment system hardware is mounted on all LOS fixtures. There will be 13 alignment paths on the CSCs (8 edge paths and 5 internal "volume" paths) and 4 alignment paths on the CSC support frames. Four LOS on the CSCs and 2 LOS on the frame will be observable with the theodolite system at all times. The following experimental tests will be conducted.
Stability tests will be made by monitoring all active channels for stability and movement over a period of 1 - 2 weeks. Personnel in the area will be kept to a minimum during the day and the hi-bay doors closed. The data acquisition rate will be approximately 15 frames stored and analyzed over a 15 second period (to average out effects of air turbulence) per alignment channel.

Software will rapidly analyze the frames and store $x$-$y$ positions at the detector for every channel, requiring well under 5 minutes to scan 17 channels.

Tests of rapid swings in temperature will be accomplished by opening up the hi-bay doors at the peak outside temperature point of the day (~ 25º C - 38º C around 14:00 during late summer). Opening and closing the doors can simulate the amount of temperature variation realized during different assembly and installation stages of the GEM muon system. Temperature monitoring with strategically placed thermocouples will be necessary for all experiments.

CSC alignment will be tested by *intentionally* moving the CSCs out of alignment to study how well all channels of the projective alignment system measure the misalignment. This is envisioned as in-plane $x$ and $y$ translations during initial testing, but would eventually include rotations and torques (twists) of all three CSCs.

Mechanical vibrations will be purposely induced into the system to study the effects on alignment stability. Monitoring of various frequencies at various input locations and coupling to alignment and monitoring components will yield valuable information especially in detecting unforeseen vibrational problems. This will be useful in defining which vibrational forcing functions must be avoided during the operation of the detector.

The merits of hardware innovations that have the potential for simplification and/or cost savings will be evaluated. There are currently 2304 LOS in the GEM muon system baseline design, providing incentive to reduce the cost of the system if possible and to simplify the design while meeting all the performance requirements. Design improvements will evolve from actual experience with the hardware.

The proposed remote CSC positioning actuators will be developed and tested. Actuators will be implemented and evaluated at all potential locations for remote actuation along with algorithms for closed loop control via feedback of position from the alignment monitors.

We will also develop, test and evaluate procedures for positioning and surveying the CSCs to each other within an alignment tower. Various procedures will be evaluated to provide the simplest and most cost effective methods.

## ACKNOWLEDGEMENTS

This work was performed under the auspices of the US Department of Energy by the Lawrence Livermore National Laboratory under Contract W-7405-ENG-48.

## REFERENCES

[1] "GEM Technical Design Report," GEM-TN-93-262, April 30, 1992.

[2] P. Duinker et. al., "Some Methods for Testing and Optimizing Proportional Wire Chambers," *Nuc. Inst. and Methods,* A273 (1988), pp. 814-819.

[3] J. A. Paradiso, D. B. Goodwin, "Wide-Range Precision Alignment for the GEM Muon System," these proceedings.

[4] G. Mitsehnakher and A. Ostapchuk, "New Approach to Muon System Alignment," GEM-TN-92-202.

[5] J. A. Paradiso, "Analysis of an Alignment Scheme for the GEM Muon Barrel," GEM-TN-92-150.

[6] G. Mitsehnakher and A. Ostapchuk, "Alignment Requirements for the GEM Muon System," GEM-TN-93-333.

[7] J. A. Paradiso, "Alignment Requirements for the GEM Muon Detector," GEM-TN-92-125.

[8] G. Mitselmakher and V. Zhukov, "Alignment Requirements to Muon System," GEM-TN-92-120.